

<https://doi.org/10.1038/s43247-024-01874-x>

No paleoclimatic anomalies are associated with the late Eocene extraterrestrial impact events

Check for updates

Bridget S. Wade & Natalie K. Y. Cheng

Two distinct extraterrestrial impacts events struck the Earth less than 25,000 years apart in the late Eocene, approximately 35.65 million years ago. These resulted in the Popigai (northern Siberia) and Chesapeake Bay (eastern North America) impacts structures, the largest of the Cenozoic era. To examine the paleoclimatic consequences attributed to the late Eocene Chesapeake and Popigai extraterrestrial impact events, we present multispecies planktonic and benthic foraminiferal oxygen ($\delta^{18}\text{O}$) and carbon ($\delta^{13}\text{C}$) isotope records. Here we generate data from the Gulf of Mexico, Deep Sea Drilling Project Site 94 covering 35.85 to 35.49 million years ago. No isotopic anomalies or excursions were recorded across the impact horizons. However, $\sim 100,000$ years before the impacts, a negative 0.75‰ $\delta^{18}\text{O}$ shift occurs in planktonic foraminifera, coincident with a 0.25‰ positive change in benthic foraminifera. We interpret this as a warming of $\sim 2^\circ\text{C}$ in the surface ocean, accompanied by 1°C deep water cooling, but these modifications are before and not coeval with the impact horizons. Despite the close succession of two or more large extraterrestrial impact events within a short space of time (less than 25,000 years), our study from the Gulf of Mexico indicates no detectable paleoclimatic response.

The late Eocene was a period of climatic change, where the Earth's descent into an icehouse world was well-underway in the form of deep ocean cooling and ephemeral glaciations in Antarctica¹. During the late Eocene, the Earth received heightened amounts of extraterrestrial matter as indicated by the discovery of numerous impact craters and an elevated helium-3 influx that lasted over 2 myr^{2–5}. Marine and terrestrial sediments across multiple geographical locations worldwide bear the imprints of two distinct impact events of late Eocene age. Geochemical and biostratigraphic data have associated the two horizons with the Popigai (northern Siberia) and the Chesapeake Bay (eastern North America) impact structures. These are the two largest known impact craters of the Cenozoic^{5–7} with diameters of ca. 100 and 40–85 km, respectively^{5,8–10}. These two separate bolide events occurred within <25 kyr of each other^{11–13} and each event generated approximately 1 billion metric tons of silicate glass spherules that were deposited as distal impact ejecta material¹⁴. Geochemical evidence suggests that these impacts most likely had asteroidal origins^{4,10,15}.

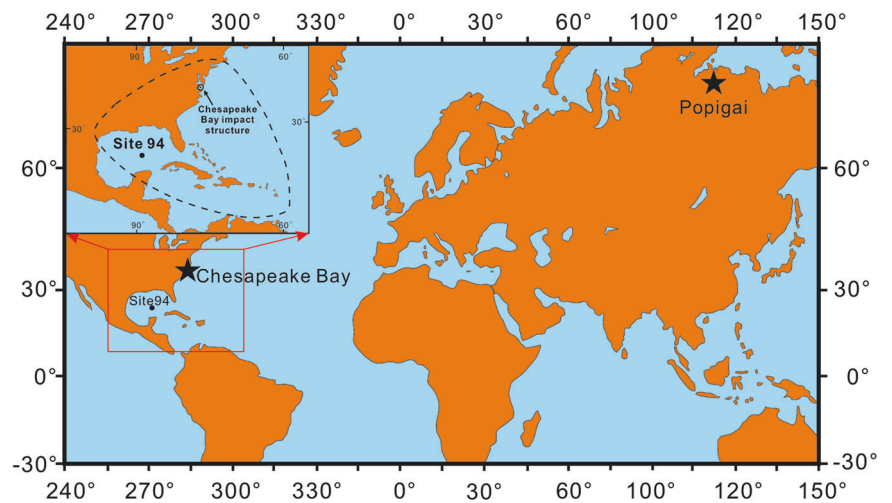
The impact event that produced the Chesapeake Bay crater has been identified as the source of the late Eocene North American (NA) tektite strewn field^{8,16}. Silicate glass bodies devoid of crystalline structures known as tektites were produced from the melting and quenching of target rocks upon impact^{14,17}. NA microtektites and tektite fragments have been discovered in land sediments and in several deep-sea sediment cores¹⁸. A separate impact ejecta layer is characterised by the presence of crystallite-bearing spherules¹⁴.

As clinopyroxene is the major crystalline phase of these spherules, they are referred to as clinopyroxene-bearing spherules or cpx spherules¹⁹. High-resolution stratigraphic analysis has made it clear that the cpx spherules belong to a separate impact ejecta layer that occurs at a stratigraphically older level (<25 kyr) compared to the NA microtektite impact horizon^{11,13,18,20}. The cpx horizon has been associated with the Popigai impact structure and the cpx layer coincides with an Ir anomaly. The Ir anomaly is another distinguishing feature of the Popigai impact horizon, as there is no Ir peak at the NA microtektite horizon^{13,14,21,22}. Cpx spherules have been observed in the northwest Atlantic Ocean, Caribbean Sea and Gulf of Mexico, where NA microtektites were also discovered^{14,23}. Cpx spherules have also been found in deep-sea sediment cores from the equatorial Pacific and Indian Oceans, as well as in the Atlantic sector of the Southern Ocean^{14,23}. The widespread geographic distribution of cpx spherules suggests that the cpx strewn field may be global in extent⁹. Further minor impact events also occurred during this time interval^{15,12,24–28}, though the age, size, extent, and correlation of other microspherule and microtektite horizons has been controversial²⁹.

That two large extraterrestrial impact events occurred in such close succession (<25 kyr) raises questions about how the planet might have responded and presents an unusual opportunity to examine the effects of these events on Earth's climate. Large impacts could release enough energy to alter climate and life on a regional or even global scale^{20,21} and thus it

Department of Earth Sciences, University College London, London, UK. ✉e-mail: b.wade@ucl.ac.uk

Fig. 1 | Location of DSDP Site 94 and the Chesapeake and Popigai impact structures. Dashed line indicates the geographic extent of the North American tektite/microtektite strewn field (redrawn after ref. 9).



would not be unreasonable to expect some environmental perturbations to occur. However, there has been controversy on the nature and direction of any environmental deviations attributed to the impact events. Prior investigations into the climatic response and effects of the late Eocene impacts have been limited to benthic and bulk carbonate stable isotope analyses^{23,30–32}, microfossil assemblages^{27,33–35} and organic molecular paleothermometer TEX₈₆³⁶. The results have been divergent about the impact-induced climatic responses, with accelerated cooling^{23,30,36}, transient warm episodes³¹ and shifts in oceanic productivity^{23,32}.

Previous studies have suggested a cooling pulse occurred near or at the impact horizons. The supporting evidence includes a fall in the abundance of shallow and warm water planktonic foraminifera species and a marked increase in a cool-water dinoflagellate species across or soon after the impact horizon at the Massignano section, Italy^{34,35}. Positive excursions in $\delta^{18}\text{O}$ values are recorded across the impact clastic layer in the Southern Ocean^{23,30}. TEX₈₆ sea surface temperatures indicate substantial (3–5°C) but transient cooling in the East Tasman Plateau and North Sea Basin, associated with magnetochron C16n.1n^{1,36}, though no microspherules were recovered at either of those sites. These findings suggest that the late Eocene impacts may have induced a period of accelerated cooling, superimposed on the general temperature decline of the late Eocene.

Conversely, some studies found evidence for a transient warming episode across the impact horizons. A short warming was suggested by a negative shift in bulk carbonate $\delta^{18}\text{O}$ values coinciding with the impact horizons at the Massignano section, Italy³¹. In Prydz Bay (Southern Ocean) mean annual temperatures derived from vegetation proxies increase across an interval correlated to the impact horizons³⁷, but in other studies no temperature change was found³². Contradictory conclusions were also drawn regarding the effects the late Eocene impacts may have had on ocean productivity. With both an increase in surface water productivity suggested³⁰ and a decrease in carbon export productivity³² across the impact horizons. Thus, no coherent story can be drawn so far regarding how the late Eocene impacts have influenced Earth's climate on the short and long term.

To explore any connection and unify our understanding of the paleoclimatic response to the late Eocene impact events, we conducted high resolution (~11 kyr) multispecies planktonic and benthic foraminiferal stable isotopic analyses across the late Eocene impact horizons from Deep Sea Drilling Project (DSDP) Site 94, Gulf of Mexico (Fig. 1). We selected this site because it exhibits the well-documented signatures of two late Eocene impacts that correspond to the NA microtektite and cpx horizons^{14,38}, as well as yielding abundant foraminiferal specimens³⁹. Our objectives were to: (1) determine the upper ocean paleoceanographic conditions related to the late Eocene impacts using multispecies planktonic foraminifera living at different ocean depths; (2) document deep ocean paleoceanographic change through a benthic foraminifera stable isotope record; (3) add to, affirm, or

amend the existing understanding of late Eocene impact-related paleoclimatic perturbations.

Results and discussion

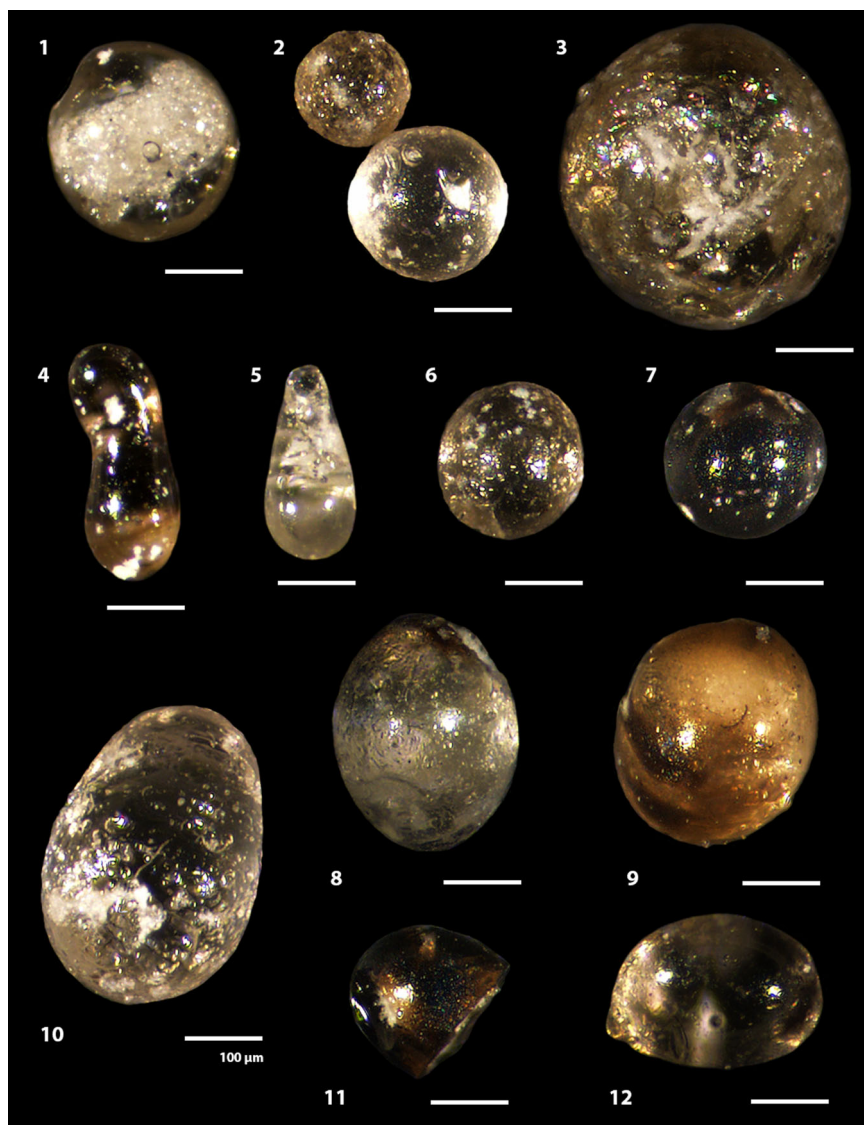
To track the number of impact microspherules across the sampled interval, and to supplement the study of ref. 14, we performed our own microspherule count from the >125 μm size fraction. Microtektites have not been distinguished from microkrystites in this study and thus all recovered spherules should be considered under the broader category of microspherules (both microtektites and crystalline-bearing microkrystites). We recovered a total of 4999 microspherules from the 26 samples (Supplementary Table 1⁴⁰). Microspherules (Fig. 2) are typical of those previously described from the late Eocene⁹. They are usually <1 mm in size, and occur primarily spherical, although ellipsoid, teardrop and dumbbell forms and fragments have also been found (Fig. 2). In most samples the microspherules count is low with less than 50 microspherules. We found a high abundance (>50 microspherules/10 cm³) between samples 15 R/3/135–137 cm and 15 R/3/89–91 cm (416.36 to 415.90 m below seafloor [mbsf]). Our peak concentration of microspherules at 15 R/3/109–111 cm (416.10 mbsf), where 3395 microspherules were recovered (Fig. 3), coincides with the younger of the two late Eocene impacts i.e., the NA microtektite horizon associated with the Chesapeake Bay impact¹⁴. The highest abundance of cpx spherules at Site 94 is 18 cm below the NA microtektite horizon at 416.28 m, associated with an Ir anomaly^{14,38} and determined to correspond to the Popigai impact event (Fig. 3)¹⁴.

Paleoceanographic change 100 kyr prior to the impact horizons

We present the first high resolution, multispecies stable isotope record from planktonic and benthic foraminifera across the late Eocene impact horizons (Fig. 3). The selection of planktonic species was made due to different calcification depths, such that our record reflects signals across various ocean habitats. We based our determination of calcification depths on published isotope analysis. *Pseudohastigerina micra* and *P. nagewichiensis* (grouped here as *Pseudohastigerina* spp.) were selected as mixed-layer dwelling species with no algal photosymbionts^{41,42}. *Turborotalia cocoaensis* was a thermocline dweller^{42–44}, and *Cibicidoides eoceanus* is a benthic form, classified as epifaunal⁴⁵.

We find evidence of paleoceanographic change in the Gulf of Mexico at a stratigraphic horizon approximately 100 kyr older than the impact events (Fig. 3). Based on the age-depth model (Supplementary Table 2), the trend started around approximately 35.75 Ma where benthic foraminifera $\delta^{18}\text{O}$ and $\delta^{13}\text{C}$ becomes more positive, and *Pseudohastigerina* $\delta^{18}\text{O}$ becomes more negative (Fig. 3). The shift is especially prominent in pseudohastigerinid $\delta^{18}\text{O}$ (−0.77‰) with a smaller change in *T. cocoaensis* (−0.39‰), indicating upper water column warming of ~2 °C. The convergence of $\delta^{18}\text{O}$ values of

Fig. 2 | Z-stacked light microscope images of microspherules from DSDP Site 94. Specimens 1, 4, 5, 12 from 15 R/3/109–111 cm; 2, 7, 8, 9, 10, 11 from 15 R/3/50–52 cm; 3, 6 from 15 R/3/31–33 cm. All scale bars = 100 μm .



Pseudohastigerina and *T. cocoaensis* suggests a disruption in water column structure, with reduced stratification. The negative planktonic foraminiferal $\delta^{18}\text{O}$ change occurs at the same time as an increase in benthic foraminifera $\delta^{18}\text{O}$ of 0.23‰, suggesting a 1 °C cooling of deep waters. The negative $\delta^{18}\text{O}$ shift in the planktonic foraminiferal record, and the positive benthic foraminifera $\delta^{18}\text{O}$ increase at 35.75 Ma, serves to expand the planktonic to benthic $\delta^{18}\text{O}$ gradient. We interpret these modifications as a cooler and younger deep water mass entering the Gulf of Mexico, accompanied by warming and greater mixing of the upper water column. After the oceanographic shift at approximately 35.75 Ma, $\delta^{18}\text{O}$ values of *Pseudohastigerina* and *T. cocoaensis* overlap and are more variable ($\pm 0.30\text{‰}$) (Fig. 3), indicating a prolonged interval of upper water column mixing. Sedimentological records from Southern Ocean sites also suggest invigoration of surface and bottom water circulation around this time¹.

No paleoceanographic anomalies at the impact horizons

We find the most positive $\delta^{18}\text{O}$ value in benthic foraminifera *C. eocaenus* of 0.79‰ occurs at 416.0 mbsf (Supplementary Table 1⁴⁰). Whilst this is the sample immediately after the NA tektite event, corresponding to the Chesapeake impact, $\delta^{18}\text{O}$ values then swiftly return to $\sim 0.5\text{‰}$ and fluctuate around this value until the top of the studied interval (Fig. 3). The stable isotope record displays no other trends that appear to correspond to the peak concentrations of NA microtektites or the Ir anomaly. Our stable isotope results from Site 94 do not record any major perturbations to the

climate or environment associated with the late Eocene impact horizons (Fig. 3). It does not appear that the paleoceanographic trends (or absence of) in our record coincide in character with the warm pulse or cooling associated with the late Eocene impact ejecta interval as reported by other studies^{23,30,31,35–37}. The oceanographic shift recorded in this investigation at 35.75 Ma (Fig. 3) does not correspond with the impact horizons and is approximately 100 kyr and 120 kyr prior to the cpx and NA tektite layers, respectively. Therefore, these paleoceanographic alterations in the Gulf of Mexico of minor deep water cooling, coupled with surface water warming and mixing are not related to the Popigai and Chesapeake impact horizons.

No clear shifts or trends in $\delta^{13}\text{C}$ were found across the dataset (Fig. 3). Our multispecies $\delta^{13}\text{C}$ record from Site 94 is unremarkable, with minimal variation and no obvious excursions to suggest a perturbation in ocean productivity across the examined interval. We find no evidence for the negative 0.5‰ $\delta^{13}\text{C}$ excursion in bulk-carbonate recognised by some previous studies^{30,32} associated with the cpx and Ir layer. The release of carbon dioxide from marine hydrates as suggested by ref. 31 should produce a global negative signal in $\delta^{13}\text{C}$ values, and no such excursion was noticeable throughout our $\delta^{13}\text{C}$ record. Therefore the $\delta^{13}\text{C}$ excursion may be short-lived, restricted to the Southern Hemisphere or not a global event.

Conclusions

Conflicting results have been drawn about the climatic and environmental effects of the late Eocene extraterrestrial impacts. While previous studies

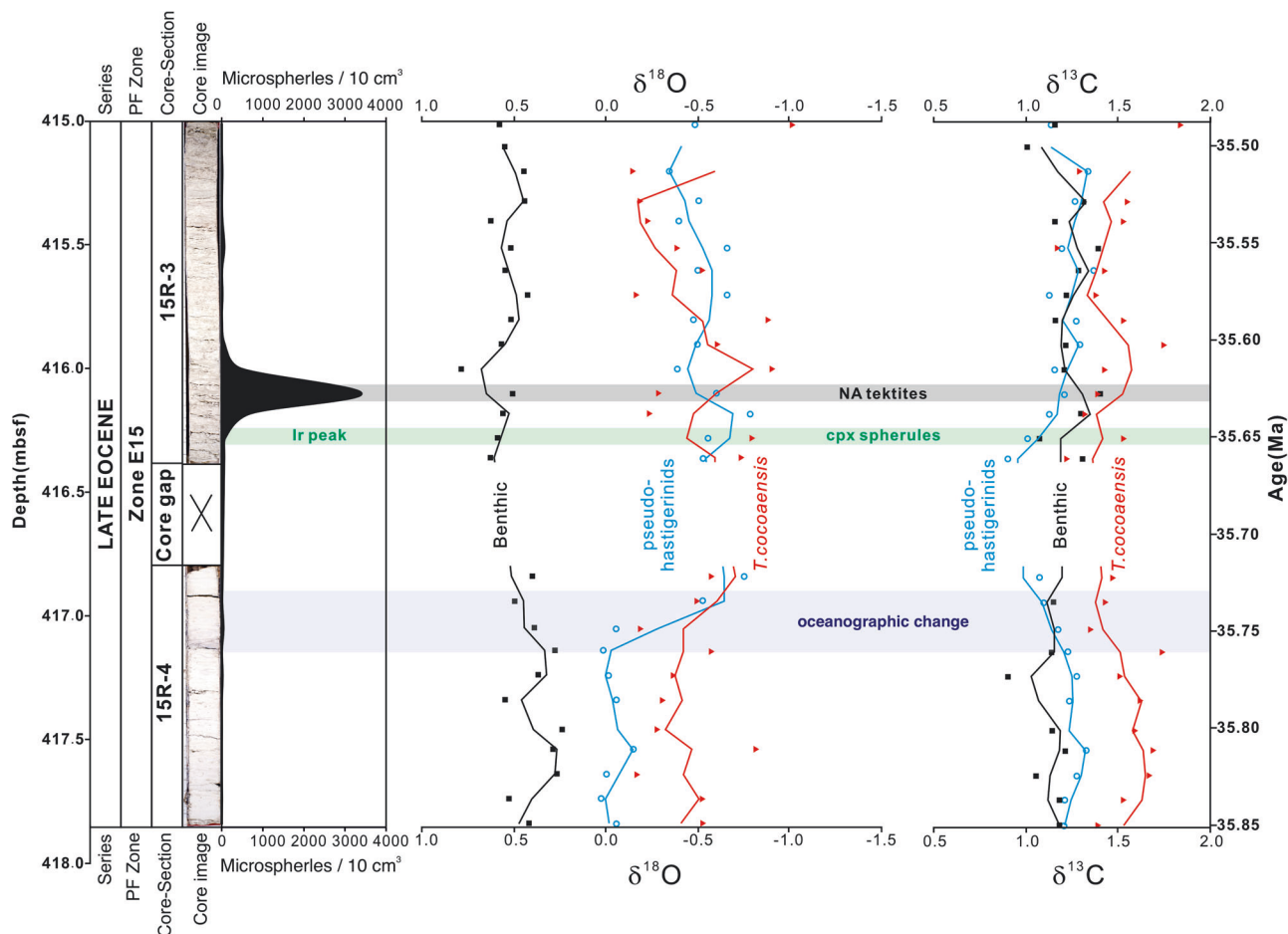


Fig. 3 | Multispecies foraminiferal stable isotopes across the late Eocene impact horizons at DSDP Site 94, Gulf of Mexico. Depth in metres below seafloor (mbsf). PF = Planktonic foraminifera zone. There is a core gap between 416.4 and 416.8 mbsf. Distribution of microspherules recovered above the 125 μm size fraction (this study). The North American microtektite layer, cpx layer and Ir peak are labelled^{14,38}. Stable isotope data of *Pseudohastigerina* spp. (*P. micra* and *P.*

naguwichiensis) (blue open circles), *Turborotalia cocoaensis* (red triangles) and benthic *Cibicidoides eocaenus* (black squares) across late Eocene impact horizons. Points are raw data, the line is a 3-point moving average. An interval of oceanographic change is highlighted, see text for discussion. Stable isotope data spans across a period of approximately 360 kyr.

have suggested accelerated cooling or warming events to have been directly induced by the late Eocene impacts, our study did not find any perturbations to the climate or to ocean productivity that correlate stratigraphically with either the NA or the cpx impact horizons. The diverging results of cooling and warming recorded in previous studies could be explained by the lower sampling resolution in former works, or global heterogeneity in climatic expression due to the invigoration of ocean currents in the late Eocene^{1,46}. We find surface water warming and deep water cooling at a stratigraphically older level, approximately 100–120 kyr before the two impact horizons. We thus conclude the absence of any climatic perturbations associated with either of the two late Eocene impact events. However, we note that whilst our sampling resolution (~11 kyr) is enhanced compared to previous investigations, modelling studies of the expected global climatic response to the K/Pg Chicxulub impact suggest radiative changes occur on much shorter timescales (<25 years)⁴⁷. Our study indicates that there is no longer term (>10 kyr) climate shift related to the close succession of extraterrestrial impacts, though shorter-term (<10 kyr) climatic response may have occurred. Although two large extraterrestrial impacts struck in close temporal space in Earth's history, they seem to have left the planet unscathed.

Materials and methods

Sample material and processing

DSDP Leg 10, Site 94 (24°31'N, 88°28'W) is situated in the Gulf of Mexico on the continental slope of the Yucatan platform (water depth of 1793 m)⁴⁸

(Fig. 1). The core consists of foraminiferal nannofossil ooze. Our study from Site 94, Core 15, Sections 3 and 4 spans 2.8 m and covers the late Eocene impact ejecta interval. Both cpx spherules and microtektites have been found at Site 94. A previous study¹⁴ sampled core 15 of Site 94 and recovered over 8500 impact spherules across the impact layer zone. They delineated the separate NA microtektite horizon and the cpx spherule horizon, with the highest abundance of cpx spherules at 416.28 m, at the same depth of an Ir anomaly¹⁴.

Twenty-six 10 cm³ samples from Site 94, core 15, Sections 3 and 4 were examined at 10 cm-intervals (417.84–415.01 mbsf). The sedimentary material was soaked in distilled water and washed under running water through a 63 μm sieve and oven dried at <40 °C. Samples were then re-washed and dried using the same method. Foraminifera are abundant and recrystallised. Calcite precipitation is observed on microspherules in some samples.

High resolution multispecies stable isotope analysis

For each sample, a total of three foraminiferal species that correspond to different ecological habitats were selected for isotope analysis. Specimens of *P. micra* and *P. naguwichiensis* were selected from the 125–250 μm size fraction and *T. cocoaensis*, and *C. eocaenus* were selected from the >250 μm size fraction. Specimens that had infilling or showed heavy calcification were avoided. All foraminifera were ultrasonicated for 2 s prior to isotopic analyses.

Foraminifera were analysed at the Bloomsbury Environmental Isotope Facility (BEIF) at University College London on a Thermo DeltaPLUS XP continuous-flow Gas-ratio mass spectrometer attached to a Thermo Gas Bench II device. Precision of all internal (BDH) and external standards (NBS-19) is $\pm 0.06\text{‰}$ for $\delta^{13}\text{C}$ and $\pm 0.10\text{‰}$ for $\delta^{18}\text{O}$ for the planktonic foraminiferal samples, and $\pm 0.02\text{‰}$ for $\delta^{13}\text{C}$ and $\pm 0.06\text{‰}$ for $\delta^{18}\text{O}$ for the benthic foraminiferal samples. All isotope values are normalised to NBS-19 and reported in per mil in the δ notation relative to the Vienna Pee Dee Belemnite (VPDB) (Supplementary Table 1⁴⁰).

The variability in the $\delta^{18}\text{O}$ record is relatively low (Fig. 3). The range between maximum and minimum $\delta^{18}\text{O}$ values in *Pseudohastigerina*, *T. cocoaensis* and *C. eoacaenus* are 0.79, 0.76 and 0.55‰, respectively. Benthic foraminifera *C. eoacaenus* $\delta^{18}\text{O}$ fluctuates between 0.24 and 0.79‰, with more negative values at the base of the studied section, increasing by 0.23‰ at 416.94 mbsf. From the bottom of the studied interval until ~417.0 mbsf, pseudohastigerinids and *T. cocoaensis* $\delta^{18}\text{O}$ are separated by approximately 0.40‰. However, $\delta^{18}\text{O}$ values converge at ~417.0 mbsf, caused by a negative shift of 0.77‰ in *Pseudohastigerina* $\delta^{18}\text{O}$ values across depths 417.14 to 416.84 mbsf, corresponding to a 40 kyr interval. Our benthic record does not reflect this trend, and benthic $\delta^{18}\text{O}$ values increase by 0.12‰. Pseudohastigerinids record $\delta^{18}\text{O}$ signatures 0.50‰ more positive than *Turborotalia cocoaensis* in the lower (older) part of our record, possibly reflecting a habitat shift in pseudohastigerinids.

Carbon isotope values of *Pseudohastigerina*, *T. cocoaensis*, and *C. eoacaenus* show minimal variability across the sampled interval (Fig. 3). Benthic *C. eoacaenus* $\delta^{13}\text{C}$ varies between 0.91 and 1.40‰. There is a trend to more positive values in the younger sediments. Pseudohastigerinid $\delta^{13}\text{C}$ varies between 0.90 and 1.38‰ and *T. cocoaensis* fluctuates by 0.67‰ between 1.18 and 1.85‰. Planktonic foraminifera *Pseudohastigerina* and *T. cocoaensis* have consistent trends in $\delta^{13}\text{C}$ (Fig. 3) with a 0.35‰ offset. The $\delta^{13}\text{C}$ difference between benthic foraminifera *C. eoacaenus* and planktonic foraminifera *Pseudohastigerina* changes through the dataset. At the bottom of the sampled interval (417.84–417.05 mbsf) benthic foraminifera $\delta^{13}\text{C}$ is more negative than *Pseudohastigerina* by 0.10‰. However, this relationship alters at 416.94 mbsf (35.73 Ma), and benthic foraminifera $\delta^{13}\text{C}$ are more positive than *Pseudohastigerina* by 0.06‰. The change to more positive benthic $\delta^{13}\text{C}$ corresponds with enhanced benthic $\delta^{18}\text{O}$ values and a negative shift in *Pseudohastigerina* $\delta^{18}\text{O}$.

Depth habitats

Ecological and environmental preferences influence the stable isotopic values of foraminifera. The stable isotope signal of planktonic foraminifera reflects where the foraminifera calcify in the water column. As $\delta^{18}\text{O}$ is temperature-dependent, species that reside in the warmer surface waters will have more negative $\delta^{18}\text{O}$ values than forms that have a deeper depth habitat. Carbon isotopes also vary through the water column. Photosynthesis in surface layers preferentially removes the ^{12}C from the ambient water, while respiration and bacterial activity reintroduces ^{12}C back into the deeper waters, thus producing a decreasing carbon isotopic profile down the water column. Size-related metabolic fractionation is also known to affect the $\delta^{13}\text{C}$ in smaller-sized foraminifera (i.e., those that are <150 μm), producing $\delta^{13}\text{C}$ values are more negative than in the larger forms^{49–51}.

Our $\delta^{13}\text{C}$ to $\delta^{18}\text{O}$ profile is in generally good agreement with the previously published ecological trends of different depth habitats. *Pseudohastigerina micra* and *P. naguwichiensis* have relatively negative $\delta^{13}\text{C}$ signatures for a planktonic foraminiferal species, plotting close to benthic foraminiferal *C. eoacaenus* values. The results are consistent with the isotopic characteristics of the small-sized (<150 μm) foraminifera such as members of the genus *Pseudohastigerina* incorporating metabolic light carbon into their tests. This pattern of depleted $\delta^{13}\text{C}$ has been observed in many small sized foraminifera, such as late Oligocene *Cassigerinella chipolensis*, *Globigerinita juvenilis*, *Tenuitella munda*⁵¹, and consistent with previous observations of *Pseudohastigerina* from the middle-late Eocene and early Oligocene^{41,42,52–54}. However, in terms of $\delta^{18}\text{O}$ profiles, previous studies from the from Tanzania suggested that pseudohastigerinids had an upper mixed-

layer habitat^{41,42,54}, but our data indicate a deeper depth. Pseudohastigerinids with more positive $\delta^{18}\text{O}$ than co-occurring turborotaliids were also recorded from Eureka E67-128 (Gulf of Mexico) and Site 366 (equatorial Atlantic)⁵². The shift to more negative $\delta^{18}\text{O}$ could reflect a shoaling in depth habitat of pseudohastigerinids as suggested by ref. 53.

Age Model

We use the Shipboard biostratigraphy⁴⁸, augmented with postcruise biostratigraphy²⁷ to produce an age-depth model and update the planktonic foraminiferal biostratigraphy to the astromagnetostratigraphy of ref. 55 (Supplementary Table 2). All sediments studied are younger than Top *Globigerinatheka semiinvoluta* and thus the entire studied record is within the *Globigerinatheka index* Highest Occurrence Zone (Zone E15)^{56,57}. The biostratigraphy is very consistent with studies from the Massignano section (Italy)⁵⁸. Based on our age-depth model, our 2.8 m sampled section stretches over a period of approximately 360 kyr from 35.85 to 35.49 Ma. This gives a temporal resolution of ~11 kyr between samples. A sedimentary void is present at the base of 15R-3 and the top of 15R-4 between depths of 416.4 m and 416.8 m, resulting in a sampling gap.

Although the cpx layer has not been radiometrically dated, magnetostratigraphic studies indicate that the cpx spherule layer and accompanying Ir anomaly occurs within mid magnetochron 16n.1n^{23,32,59}, indicating a magnetochronologic age of 35.43 Ma (as per ref. 60). The revised age for C16n.1n as per ref. 55 (which is also consistent with GTS2020⁶¹) is 35.718–35.580 Ma, suggesting a magnetochronologic age of the cpx event as 35.65 Ma. The Popigai impact crater has been dated through the ⁴⁰Ar/³⁹Ar method and found to have an age of 35.7 \pm 0.2 Ma⁶². The radiometric age of the Popigai crater is thus consistent with the revised magnetostratigraphic derived ages of the cpx layer.

The Site 94 age model indicates the NA microtektite layer at 416.1 m has an age of 35.63 Ma, which is in good agreement of radiometric dates of 35.4 \pm 0.6 Ma, 35.5 \pm 0.3 Ma, 35.3 \pm 0.2 Ma by refs. 63–65, respectively. Previous biostratigraphic studies indicate that the cpx layer is ~10–20 kyr older than the NA microtektite layer^{5,11,20,22}. The temporal separation between the two horizons in our study is 23 kyr.

The extraterrestrial impact interval (Sections 3 and 4 of core 15) bears no signs of sediment reworking or unconformity⁴⁸. A hiatus was suggested in 15R-4 by ref. 39 however, this was based on the close succession of the extinction of *Globigerinatheka semiinvoluta* and the base of *Turborotalia cunialensis* (*Globorotalia cerroazulensis cunialensis* in ref. 39). However, the base of *T. cunialensis* is problematic due to taxonomic inconsistencies between authors and differentiating *T. cunialensis* from other species within the *Turborotalia* genus⁵⁶. Thus the base of *T. cunialensis* was not used in more recent zonations^{56,57} and we excluded this bioevent from our age model (Supplementary Table 2). Our updated age model and new sediment core images do not indicate a hiatus.

Data availability

The foraminifera stable isotope data and microspherule counts generated in this study are provided in Supplementary Table 1. These data are also uploaded to the NERC EDS National Geoscience Data Centre (<https://doi.org/10.5285/a0b6a773-1d18-4ced-a57e-06f8d67428b9>)⁴⁰.

Received: 28 April 2024; Accepted: 4 November 2024;

Published online: 04 December 2024

References

- Houben, A. J. P. et al. Late Eocene Southern Ocean cooling and invigoration of circulation preconditioned Antarctica for full-scale glaciation. *Geochem. Geophys. Geosyst.* **20**, 2214–2234 (2019).
- Farley, K. A. Cenozoic variations in the flux of interplanetary dust recorded by ³He in a deep-sea sediment. *Nature* **376**, 153–156 (1995).
- Farley, K. A. et al. Geochemical evidence for a comet shower in the late Eocene. *Science* **280**, 1250–1253 (1998).

4. Schmitz, B. et al. Fragments of Late Eocene Earth-impacting asteroids linked to disturbance of asteroid belt. *Earth Planet. Sci. Lett.* **425**, 77–83 (2015).
5. Koeberl, C. Late Eocene impact craters and impactoclastic layers—An overview. *Geol. Soc. Am. Spec. Pap.* **452**, 17–26 (2009).
6. Poag, W. et al. The Chesapeake Bay Crater: Geology and Geophysics of a Late Eocene Submarine Impact Structure, (Springer Science & Business Media, 2004).
7. Gohn, G. et al. Deep drilling into the Chesapeake Bay impact structure. *Science* **320**, 1740–1745 (2008).
8. Poag, C. W. et al. Meteoroid mayhem in Ole Virginny: source of the North American tektite strewn field. *Geology* **22**, 691–694 (1994).
9. Glass, B. P. & Simonson, B. M. Distal impact ejecta layers: a record of large impacts in sedimentary deposits, (Springer Sci. Bus. Media, 2013).
10. Boschi, S. et al. Late Eocene ³He and Ir anomalies associated with ordinary chondritic spinels. *Geochim. Cosmochim. Acta* **204**, 205–218 (2017).
11. Glass, B. P. et al. Upper Eocene tektite and impact ejecta layer on the continental slope off New Jersey. *Meteorit. Planet. Sci.* **33**, 229–241 (1998).
12. Whitehead, J. et al. Late Eocene impact ejecta: Geochemical and isotopic connections with the Popigai impact structure. *Earth Planet. Sci. Lett.* **181**, 473–487 (2000).
13. Kyte, F.T. & Liu, S. Iridium and spherules in late Eocene impact deposits (abstr. 1981). In *32nd Lunar and Planetary Science Conference* (Lunar and Planetary Institute, 2002).
14. Glass, B. P. et al. Late Eocene North American microtektites and clinopyroxene-bearing spherules. *J. Geophys. Res. Solid Earth* **90**, 175–196 (1985).
15. Koeberl, C. et al. Late Eocene impact ejecta in Italy: attempts to constrain the impactor composition from isotopic analyses of spinel-rich samples. *Geol. Soc. Am. Spec. Pap.* **542**, 347–354 (2019).
16. Koeberl, C. et al. Impact origin of the Chesapeake Bay structure and the source of the North American tektites. *Science* **271**, 1263–1266 (1996).
17. Keller, G. et al. Multiple impacts across the Cretaceous–Tertiary boundary. *Earth-Sci. Rev.* **62**, 327–363 (2003).
18. McCall, G. J. H. Tektites in the geological record: showers of glass from the sky, (Geological Society, 2001).
19. Glass, B. P. & Burns, C. A. Microkrystites—a new term for impact-produced glassy spherules containing primary crystallites (abstr.). In *18th Lunar and Planetary Science Conference*. 455–458 (Lunar and Planetary Institute, 1988).
20. Sanfilippo, A. et al. Late Eocene microtektites and radiolarian extinctions on Barbados. *Nature* **314**, 613–615 (1985).
21. Alvarez, W. et al. Iridium anomaly approximately synchronous with terminal Eocene extinction. *Science* **216**, 886–888 (1982).
22. Glass, B. P., DuBols, D. L. & Ganapathy, R. Relationship between an iridium anomaly and the North American microtektite layer in core RC9-58 from the Caribbean Sea. *J. Geophys. Res.* **87**, 425–428 (1982).
23. Liu, S. et al. The late Eocene clinopyroxene-bearing spherule layer: New sites, nature of the strewn field, Ir data, and discovery of coesite and shocked quartz. *Geol. Soc. Am. Spec. Pap.* **452**, 37 (2009).
24. Keller, G., D'Hondt, S. L. & Vallier, T. L. Multiple microtektite horizons in upper Eocene marine sediments: no evidence for mass extinction. *Science* **221**, 150–152 (1983).
25. Keller, G. et al. Late Eocene impact microspherules: stratigraphy, age and geochemistry. *Meteoritics* **22**, 25–60 (1987).
26. Hazel, J. E. Chronostratigraphy of upper eocene microspherules. *Palaios* **4**, 318–329 (1989).
27. Molina, E., Gonzalvo, C. & Keller, G. The Eocene–Oligocene planktic foraminiferal transition: extinctions, impacts and hiatuses. *Geol. Mag.* **130**, 483–499 (1993).
28. Montanari, A., Bagatin, A. C. & Farinella, P. Earth cratering record and impact energy flux in the last 150. *Ma. Planet. Space Sci.* **46**, 271–281 (1998).
29. Glass, B. P. Chronostratigraphy of upper eocene microspherules: comment & reply. *Palaios* **5**, 387–390 (1990).
30. Vonhof, H. B. et al. Global cooling accelerated by early late Eocene impacts? *Geology* **28**, 687–690 (2000).
31. Bodiselišch, B. et al. Delayed climate cooling in the Late Eocene caused by multiple impacts: high-resolution geochemical studies at Massignano, Italy. *Earth Planet. Sci. Lett.* **223**, 283–302 (2004). (3–4).
32. Pusz, A. E. et al. Stable isotopic response to late Eocene extraterrestrial impacts. *Geol. Soc. Am. Spec. Pap.* **452**, 83–95 (2009).
33. Molina, E. et al. Foraminiferal turnover across the Eocene–Oligocene transition at Fuente Caldera, southern Spain: No cause–effect relationship between meteorite impacts and extinctions. *Marine Micropaleontol.* **58**, 270–286 (2006).
34. Coccioni, R. et al. Marine biotic signals across a late Eocene impact layer at Massignano, Italy: evidence for long-term environmental perturbations? *Terra Nova* **12**, 258–263 (2000).
35. Spezzaferri, S. et al. Late Eocene planktonic foraminiferal response to an extraterrestrial impact at Massignano GSSP (Northeastern Appennines, Italy). *J. Foram. Res.* **32**, 188–199 (2002).
36. Śliwińska, K. et al. Climate- and gateway-driven cooling of Late Eocene to earliest Oligocene sea surface temperatures in the North Sea Basin. *Sci. Rpts.* **9**, 4458 (2019).
37. Passchier, S. et al. An Antarctic stratigraphic record of stepwise ice growth through the Eocene–Oligocene transition. *GSA Bull.* **129**, 318–330 (2017).
38. Glass, B. P. & Zwart, M. North American microtektites in Deep Sea Drilling Project cores from the Caribbean Sea and Gulf of Mexico. *Geol. Soc. Am. Bull.* **90**, 595–602 (1979).
39. Keller, G. Eocene and Oligocene stratigraphy and erosional unconformities in the Gulf of Mexico and Gulf Coast. *J. Paleontol.* **58**, 882–903 (1985).
40. Wade, B. & Cheng, N. Late Eocene microspherule count and foraminifera multispecies oxygen and carbon stable isotope data from DSDP Site 94. NERC EDS National Geoscience Data Centre. (Dataset). <https://doi.org/10.5285/a0b6a773-1d18-4ced-a57e-06f8d67428b9> (2024).
41. Pearson, P. N. et al. Warm tropical sea surface temperatures in the Late Cretaceous and Eocene epochs. *Nature* **413**, 481–487 (2001).
42. Wade, B. S. & Pearson, P. N. Planktonic foraminiferal turnover, diversity fluctuations and geochemical signals across the Eocene/Oligocene boundary in Tanzania. *Mar. Micropaleontol.* **68**, 244–255 (2008).
43. Wade, B. S. Planktonic foraminiferal biostratigraphy and mechanisms in the extinction of *Morozovella* in the late Middle Eocene. *Mar. Micropaleontol.* **51**, 23–38 (2004).
44. Aze, T. et al. A phylogeny of Cenozoic macroperforate planktonic foraminifera from fossil data. *Biol. Rev.* **86**, 900–927 (2011).
45. Katz, M. E. et al. Early Cenozoic benthic foraminiferal isotopes: Species reliability and interspecies correction factors. *Paleoceanography* **18**, 1024 (2003).
46. Miller, K. G. et al. Climate threshold at the Eocene–Oligocene transition: Antarctic ice sheet influence on ocean circulation. *Geol. Soc. Am. Spec. Pap.* **452**, 1–10 (2009).
47. Senel, C. B. et al. Chicxulub impact winter sustained by fine silicate dust. *Nature Geoscience* **16**, 1033–1040 (2023).
48. Worzel, J. L. et al. in *Initial Reports of the Deep Sea Drilling Project 195–258* (U.S. Government Printing Office, 1973).
49. Norris, R. D. Symbiosis as an evolutionary innovation in the radiation of Paleocene planktic foraminifera. *Paleobiology* **22**, 461–480 (1996).
50. Bornemann, A. & Norris, R. D. Size-related stable isotope changes in Late Cretaceous planktic foraminifera: implications for paleoecology and photosymbiosis. *Mar. Micropaleontol.* **65**, 32–42 (2007).

51. Pearson, P. N. & Wade, B. S. Taxonomy and stable isotope paleoecology of well-preserved planktonic foraminifera from the uppermost Oligocene of Trinidad. *J. Foram. Res.* **39**, 191–217 (2009).
 52. Poore, R. Z. & Matthews, R. K. in *Initial Reports of the Deep Sea Drilling Project 73* (eds Hsü, K. J. et al.) 725–735 (U.S. Government Printing Office, 1984).
 53. Boersma, A., Premoli Silva, I. & Shackleton, N. J. Atlantic Eocene planktonic foraminiferal paleohydrographic indicators and stable isotope paleoceanography. *Paleoceanography* **2**, 287–331 (1987).
 54. Pearson, P. N. & Wade, B. S. Systematic taxonomy of exceptionally well-preserved planktonic foraminifera from the Eocene/Oligocene boundary of Tanzania. *Cushman Found. Foram. Res. Spec. Publ.* **45**, 1–85 (2015).
 55. Westerhold, T. et al. Orbitally tuned timescale and astronomical forcing in the middle Eocene to early Oligocene. *Climate Past* **10**, 955–973 (2014).
 56. Berggren, W. A. & Pearson, P. N. A revised tropical to subtropical Paleogene planktonic foraminiferal zonation. *J. Foram. Res.* **35**, 279–298 (2005).
 57. Wade, B. S. et al. Review and revision of Cenozoic tropical planktonic foraminiferal biostratigraphy and calibration to the geomagnetic polarity and astronomical time scale. *Earth-Sci. Rev.* **104**, 111–142 (2011).
 58. Coccioni, R., Frontalini, F. & Spezzaferri, S. Late Eocene impact-induced climate and hydrological changes: Evidence from the Massignano global Stratotype section and point (central Italy). *Geol. Soc. Am. Spec. Pap.* **452**, 97–118 (2009).
 59. Jovane, L. et al. Eocene–Oligocene paleoceanographic changes in the stratotype section, Massignano, Italy: Clues from rock magnetism and stable isotopes. *J. Geophys. Res.* **112**, B11101 (2007).
 60. Cande, S. C. & Kent, D. V. Revised calibration of the geomagnetic polarity timescale for the Late Cretaceous and Cenozoic. *J. Geophys. Res.* **100**, 6093–6095 (1995).
 61. Speijer, R. P. et al. The Paleogene Period, in *Geologic Time Scale 2020*, (Elsevier, 2020).
 62. Bottomley, R. et al. The age of the Popigai impact event and its relation to events at the Eocene/Oligocene boundary. *Nature* **388**, 365–368 (1997).
 63. Glass, B. P., Hall, C. & York, D. $^{40}\text{Ar}/^{39}\text{Ar}$ laser-probe dating of North American tektite fragments from Barbados and the age of the Eocene–Oligocene boundary. *Chem. Geol. Isotope Geoscience section* **59**, 181–186 (1986).
 64. Obradovich, J., Snee, L. & Izett, G. Is there more than one glassy impact layer in the late Eocene? (abstr.). In *Geological Society of America Abstracts with Programs* A134 (Geological Society of America, 1989).
 65. Horton, J. W. & Izett, G. A. in *Studies of the Chesapeake Bay Impact Structure: U.S. Geological Survey Professional Paper* (eds Horton, J. W., Powars, D. S. & Gohn, G. S.) E1–E30 (U.S. Geological Survey, 2005).
- Deep Sea Drilling Project sample request 059652IODP. The International Ocean Discovery Program and its predecessors is sponsored by the U.S. National Science Foundation and participating countries. We thank Vincent Percuoco for providing core images of Site 94, Anne-Lise Jourdan for assistance with isotope analysis in the Bloomsbury Environmental Isotope Facility (BEIF), Pieter Vermeesch for discussion of Ar/Ar decay constants, Zheyu Tian for making Figs. 1 and 3, and Paul Pearson for discussion of age models and comments on figures and an earlier draft. B.S.W. was supported by UK Natural Environment Research Council (NERC) grant NE/V018361/1.

Author contributions

N.K.Y.C. generated the data under supervision of B.S.W. B.S.W. and N.C. conducted the analysis and wrote the paper.

Competing interests

The authors declare no competing interests.

Additional information

Supplementary information The online version contains supplementary material available at <https://doi.org/10.1038/s43247-024-01874-x>.

Correspondence and requests for materials should be addressed to Bridget S. Wade.

Peer review information *Communications Earth & Environment* thanks Christian Koeberl, Andrew Fraass and Kenneth Miller for their contribution to the peer review of this work. Primary Handling Editors: Sze Ling Ho and Carolina Ortiz Guerrero. A peer review file is available

Reprints and permissions information is available at <http://www.nature.com/reprints>

Publisher's note Springer Nature remains neutral with regard to jurisdictional claims in published maps and institutional affiliations.

Open Access This article is licensed under a Creative Commons Attribution 4.0 International License, which permits use, sharing, adaptation, distribution and reproduction in any medium or format, as long as you give appropriate credit to the original author(s) and the source, provide a link to the Creative Commons licence, and indicate if changes were made. The images or other third party material in this article are included in the article's Creative Commons licence, unless indicated otherwise in a credit line to the material. If material is not included in the article's Creative Commons licence and your intended use is not permitted by statutory regulation or exceeds the permitted use, you will need to obtain permission directly from the copyright holder. To view a copy of this licence, visit <http://creativecommons.org/licenses/by/4.0/>.

© The Author(s) 2024

Acknowledgements

We are grateful to Christian Koeberl, Andy Fraass and Ken Miller for insightful reviews that improved the manuscript. This study used samples from the